# Permeant Ion Effects on the Gating Kinetics of the Type *L* Potassium Channel in Mouse Lymphocytes

MARK S. SHAPIRO and THOMAS E. DECOURSEY

From the Department of Physiology, Rush Medical Center, Chicago, Illinois 60612

ABSTRACT Permeant ion species was found to profoundly affect the gating kinetics of type *l* $K^+$ currents in mouse T lymphocytes studied with the whole-cell or on-cell patch gigaohm-seal techniques. Replacing external $K^+$ with $Rb^+$ (as the sole monovalent cation, at 160 mM) shifted the peak conductance voltage (*g-V*) relation by ~20 mV to more negative potentials, while $NH_4^+$ shifted the *g-V* curve by 15 mV to more positive potentials. Deactivation (the tail current time constant, $\tau_{tail}$) was slowed by an average of 14-fold at −70 mV in *external* $Rb^+$, by ~8-fold in $Cs^+$, and by a factor of two to three in $NH_4^+$. Changing the external $K^+$ concentration, $[K^+]_o$, from 4.5 to 160 mM or $[Rb^+]_o$ from 10 to 160 mM had no effect on $\tau_{tail}$. With all the *internal* $K^+$ replaced by $Rb^+$ or $Cs^+$ and either isotonic $Rb^+$ or $K^+$ in the bath, $\tau_{tail}$ was indistinguishable from that with $K^+$ in the cell. With the exception of $NH_4^+$, activation time constants were insensitive to permeant ion species. These results indicate that external permeant ions have stronger effects than internal permeant ions, suggesting an external modulatory site that influences $K^+$ channel gating. However, in bi-ionic experiments with reduced external permeant ion concentrations, $\tau_{tail}$ was sensitive to the direction of current flow, indicating that the modulatory site is either within the permeation pathway or in the outer vestibule of the channel. The latter interpretation implies that outward current through an open type *l* $K^+$ channel significantly alters local ion concentrations at the modulatory site in the outer vestibule, and consequently at the mouth of the channel. Experiments with mixtures of $K^+$ and $Rb^+$ in the external solution reveal that deactivation kinetics are minimally affected by addition of $Rb^+$ until the $Rb^+$ mole fraction approaches unity. This relationship between mole fraction and $\tau_{tail}$, together with the concentration independence of $\tau_{tail}$, was hard to reconcile with simple models in which occupancy of a site within the permeation pathway prevents channel closing, but is consistent with a model in which a permeant ion binding site in the outer vestibule modulates gating depending on the species of ion occupying the site. A description of the ionic selectivity of the type *l* $K^+$ channel is presented in the companion paper (Shapiro and DeCoursey, 1991*b*).

Address reprint requests to Dr. Thomas E. DeCoursey, Department of Physiology, Rush Medical Center, 1653 West Congress Parkway, Chicago, IL 60612.

Dr. Shapiro's present address is Department of Physiology/Biophysics, University of Washington, SJ-40, Seattle, WA 98195.

J. GEN. PHYSIOL. © The Rockefeller University Press · 0022-1295/91/06/1251/28 $2.00
Volume 97 June 1991 1251–1278

## INTRODUCTION

In contrast with the original Hodgkin-Huxley (1952) assumption that ion channel gating proceeds independently of the presence or species of permeant ion, increasing evidence now indicates that permeant ions affect gating in a variety of channel types. Permeant ions influence gating kinetics in sodium (Meves and Vogel, 1973), gramicidin (Kolb and Bamberg, 1977), amphotericin B (Ermishkin et al., 1977), inhibitory synaptic (Onodera and Takeuchi, 1979), acetylcholine receptor (AchR) channels (Van Helden et al., 1977; Ascher et al., 1978; Gage and Van Helden, 1979; Marchais and Marty, 1979; Adams et al., 1981), and delayed rectifier $K^+$ channels in nerve, muscle, and other preparations (Århem, 1980; Swenson and Armstrong, 1981; Beam and Donaldson, 1983; Cahalan and Pappone, 1983; Cahalan et al., 1985; Plant, 1986; Matteson and Swenson, 1986; Lucero and Pappone, 1989; Spruce et al., 1989). In the case of AchR channels, permeant ion species strongly modify mean open times when these ions carry the current. Furthermore, for several of the metal ions the time constant $\tau$ correlated inversely with the unitary current (derived from fluctuation analysis) for each ionic species; i.e., permeant ions with smaller conductance were associated with slower closing rates.

The reciprocal relationship between channel open lifetime and conductance suggested that this "permeant ion effect" could be explained if permeant ions occupied binding sites within the channel pore during permeation, with each ionic species having a different affinity for the binding site(s). In this "occupancy hypothesis," closing is prevented or hindered when a permeant ion is bound in the channel, thus accounting for the observed differences in closing rates (Ascher et al., 1978; Gage and Van Helden, 1979; Marchais and Marty, 1979). Adams et al. (1981) on the other hand, while confirming previous results for several of the metal ions, found no correlation between elementary conductance and $\tau$ for a large number of organic cations, and concluded that an external or internal modulatory site, not a binding site in the permeation pathway (pore), may be the mechanism involved.

The companion paper (Shapiro and DeCoursey, 1991*b*) describes the selectivity of type *l* channels, as well as providing a more thorough description of gating kinetics. Here we explore the effects on gating kinetics of permeant ion species. Several experiments were designed to provide evidence regarding possible mechanisms of these effects. In most ionic conditions, the species of ion present in the external solution appears to determine type *l* closing kinetics, but there are several examples in which gating is modified by the species of ion carrying net current. In particular, we try to discriminate between models in which the channel cannot close when occupied ("occupancy models"), and models in which the closing rate of the channel is determined by the species of ion bound to a modulatory site. The bulk of the data appear to support the idea of a modulatory site, and in addition indicate that this modulatory site is most likely located near the external mouth of the channel, either just within the permeation pathway or in the vestibule.

Preliminary accounts of this work have appeared in abstract form (Shapiro and DeCoursey, 1989; Shapiro and DeCoursey, 1991*a*).

## METHODS

The experimental methods are described in the companion paper (Shapiro and DeCoursey, 1991*b*).

### *Eyring Model*

Calculations were done with a three-barrier, two-site model, using a FORTRAN computer program, CAMOD, slightly modified from a version generously provided by the laboratory of M. D. Cahalan (University of California at Irvine, Irvine, CA). A repulsion factor of 2.0 and a frequency factor of $4.92 \times 10^{11}$/s were assumed for all calculations. In calculations based upon Matteson and Swenson (1986) parameters, barriers (in units of RT), starting from the outside, were 9.4, 8.1, 9.9 and wells −7.4, −7.1 for $K^+$ and barriers were 9.4, 8.2, 11.5 and wells −8.4, −9.7 for $Rb^+$. For both ions, wells were spaced at 0.1 and 0.9, and barriers at 0.05, 0.5, and 0.95, similar to values used by Matteson and Swenson. Different spacings were also tried, which necessitated slight adjustments of the inner $Rb^+$ well to simulate the effect of $Rb^+$ on the type *l* $\tau_{tail}$. Other sets of calculations are described in the Discussion or in the legend to Fig. 12.

### *Diffusion Model*

Local ion concentrations resulting from current flow through single $K^+$ channels were calculated using a compartmental diffusion model similar to that described by Hille (1977). Identical vestibules were assumed at each end of the channel, with dimensions given in Fig. 13. Each vestibule was divided into 30 sections each 2 Å thick. The bath outside each vestibule was divided into 20 further disks 2 Å thick, each one with a radius parallel to the plane of the membrane surface 2 Å longer than the previous one. Increasing the number of bath compartments to 30 had negligible effects on the calculated concentrations of ions in the vestibule. The "cellular" compartments and the inner vestibule were initially "filled" with the ionic constituents of the pipette solution, the outer vestibule compartments and the bath compartments were filled initially with the bath solution. Diffusion was driven by influx and efflux into the inner and outer compartments adjacent to the pore, based on an estimate of the two unidirectional components, which added together comprise the net current. As a first approximation, we used the component currents calculated with the Goldman-Hodgkin-Katz current equation (Goldman, 1943; Hodgkin and Katz, 1949), scaled according to observed or estimated single channel currents appropriate for the ionic conditions. Diffusion of $K^+$ and of $Rb^+$ were calculated separately, and we did not constrain the total concentrations. $Rb^+$ was assigned an entry rate 0.76 that of $K^+$ to reflect its lower permeability. For example, efflux of $Rb^+$ into the innermost compartment of the outer vestibule is given by: $[P_{Rb}[Rb^+]/(P_{Rb}[Rb^+] + [K^+])]i_{out}/F$ where the relative $Rb^+$ permeability $P_{Rb}$ is 0.76, the concentration term gives the mole fraction of $Rb^+$ in the compartment adjacent to the *inner* end of the pore, $i_{out}$ is the outward component of unitary current, and $F$ is Faraday's constant.

A simple Euler method as described by Hille (1977) was used. The flux, $m$, from the $n^{th}$ compartment to the $(n + 1)^{th}$ compartment is given by $m_{n,n+1} = (c_n - c_{n+1}) \cdot A_n \cdot D/\Delta x$, where $c_x$ is the concentration (in moles/cm$^3$) in the $x^{th}$ compartment, $A_n$ is the area between the $n^{th}$ and $(n + 1)^{th}$ compartments, $D$ is the diffusion coefficient of $K^+$ or $Rb^+$, and $\Delta x$ is the thickness of each compartment (in centimeters). After each increment of time, $\Delta t$, $c_n$ is increased by $(m_{n-1,n} - m_{n,n+1}) \cdot \Delta t/V_n$, where $V_n$ is the volume (in cm$^3$) of compartment $n$. For most calculations, the compartments were made 2 Å thick, and $\Delta t$ was $< 10$ ps. Making the compartments 1 Å thick gave similar results, but then $\Delta t$ had to be reduced to maintain stability of the calculation. Using much shorter $\Delta t$ did not affect the results materially. Usually the calculated concentrations in the vestibule equilibrated after 30–40 ns, consistent with the rapid diffusional equilibrium expected at this distance scale (Läuger, 1976; e.g., see Fig. 32 in Barry and Diamond, 1984).

### *Voltage Shift*

The voltage dependence of type *l* kinetics and the peak conductance voltage (*g-V*) curve were not invariant during the course of an experiment but rather tended to shift in the negative

direction during whole-cell perfusion. This shift is illustrated for a typical cell in Fig. 1 *A*, in which *g-V* curves obtained at 2 and 18 min after breaking into the cell are plotted. The *g-V* relation at 2 min has a midpoint potential, $V_{½}$, of +17 mV, determined by fitting the data with a Boltzmann function (curve in Fig. 1, see legend). The *g-V* relation at 18 min is shifted to the left by ~20 mV relative to the family at 2 min, with a $V_{½}$ of −3 mV. Typical values for the shift of $V_{½}$ after 40 min in the whole-cell configuration, quantified by estimating the voltage at which

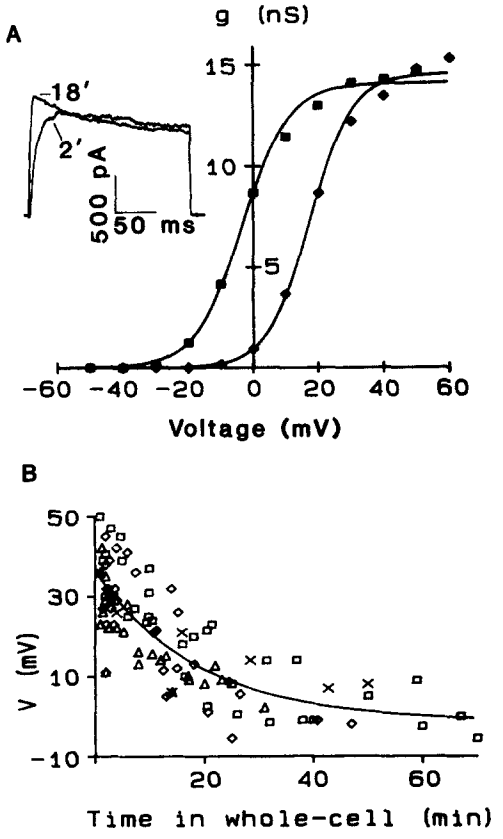


FIGURE 1. (*A*) Voltage shift of the *g-V* relation with time in whole-cell. Peak *g-V* curves at 2 min (◆) and 18 min (■) in a cell containing KF/Cl with Ringer solution in the bath. The bathing solution was not changed during this interval. Least-squares Boltzmann fit to the 2-min data is $g$ (nS) = $14.7/[1 + \exp[(17.4-V)/6.5]]$ ($V_{½}$ = 17.4 mV); to the 18-min curve is $g$ (nS) = $14.2/[1 + \exp[(-3.3-V)/7.2]]$ ($V_{½}$ = −3.3 mV). The chord conductance in Ringer solution does not completely saturate (qualitatively consistent with GHK rectification for these ionic conditions), so the fit of the data to a saturating Boltzmann is only approximate at positive potentials. Superimposed in the inset are 200-ms pulses to 30 mV from the 2- and 18-min families, as indicated. Filter 1 kHz, 22.5°C, cell No. 111. (*B*) Voltage-shift of activation time constant ($\tau_{act}$) with time in the whole-cell configuration, in many cells. The potential at which $\tau_{act}$ equals 5 ms is plotted on the ordinate against the time in whole-cell when the measurement was made. Data were corrected for temperature assuming a $Q_{10}$ of 3.5. The different symbols represent different pipette solutions: (◇) $KCH_3SO_3$; (□) $KCH_3SO_3$/F; (△) KF/Cl; (×) RbF/Cl. Most of the data are with Ringer or K-Ringer solution in the bath; there are also some points with other permeant ion species in the bath. The fit of the data to a single exponential using a nonlinear least-squares algorithm is shown as a solid line: amplitude, 38.5 mV; $\tau$, 20.4 min; steady state, −1.82 mV. No differences were seen in the voltage shift with different pipette solutions or external permeant ion species.

the *g-V* relation was half-maximal at various times, were 25–35 mV. The effect was variable; however, in no cell was the shift less than 20 mV after half an hour. The shift in $V_{½}$ can be roughly described by a single exponential, although there is a hint of a faster component during the first 5–10 min. No correlation with pipette (internal) solution could be detected; voltage shifts were seen in experiments with $K^+$ or $Rb^+$, high or low free $Ca^{2+}$ or $Mg^{2+}$, or 5 mM MgATP included in the pipette solution.

In the inset to Fig. 1 *A* are shown currents in response to identical voltage pulses to 30 mV from each family. The current recorded later shows, relative to the first: (*a*) a larger peak current consistent with increasing open probability, (*b*) faster activation, and (*c*) more pronounced inactivation during the pulse. During the progression of the experiment, longer inter-pulse intervals were needed to prevent accumulation of inactivation during successive pulses, suggesting in addition that recovery from inactivation became slower. In summary, most of the changes with time are consistent with a voltage shift reminiscent of that reported in a variety of cell types (e.g., Marty and Neher, 1983; Fernandez et al., 1984).

Fig. 1 *B* summarizes a different measure of the voltage shift in many cells in which currents were studied at various times after breaking into the cell, with different permeant ions in the bath (as well as several with $Rb^+$ in the cell). Plotted on the ordinate is the potential at which the activation time constant equals 5 ms, and on the abscissa is the time after achieving whole-cell configuration. The time course of the voltage shift is roughly exponential; superimposed on the graph is the least squares fit (amplitude = 38.5 mV, $\tau$ = 20.4 min, steady state = −1.82 mV) of an exponential to the data. The amplitude and time course of this voltage shift are similar to those seen with the voltage shifts of *g-V* curves discussed above (Fig. 1 *A*), suggesting that the two observations result from the same mechanism. The shift in voltage dependence of type *l* activation appears to occur independently of ionic conditions, at least of those studied.

This phenomenon obviously complicates quantitation of voltage-dependent parameters. If the mechanism responsible for this effect involves the loss of some intracellular cofactor from the channel milieu during the experiment, then the slow equilibration time course, with a time constant of ~20 min, indicates that this substance must be quite large (Pusch and Neher, 1988), or perhaps chemically bound to the channel. No correlation between the time course or amplitude of the voltage shift and the contents of pipette solutions was found; nothing in any of our pipette solutions would be expected to equilibrate this slowly. Much previous work has described voltage shifts seen during whole-cell clamp. A Donnan potential is presumed to exist between the pipette and cell interior caused by the slow equilibration of the more immobile negative charges in the cell (e.g., proteins) and the pipette anions. Marty and Neher (1983) calculated a maximum Donnan shift of 12 mV if all of the anions in the cell are bulky. Fernandez et al. (1984) calculated a maximum Donnan shift of 15 mV, with a larger value possible only if pipette *cations* are also immobile. Thus, at most only part of the 25–35-mV voltage shifts in our study can be ascribed to dissipation of a Donnan potential. Fernandez et al. (1984) observed voltage shifts of >25 mV in $Na^+$ channels, larger than their calculated Donnan maximum, and they concluded, as we do here, that some other process must be responsible. Furthermore, if the dissipation of a junction potential between pipette and cell caused the voltage shift, one would expect the reversal potential to shift; in fact, the reversal potential in Ringer solution shifted at most 4–5 mV during long experiments.

## RESULTS

### *Permeant Ion Effects with $K^+$ in the Cell*

*Conductance-voltage curves.* The *g-V* relation for type *l* currents was affected by the permeant ion species in the external bath. Fig. 2 shows peak *g-V* curves in the presence of 160 mM $K^+$, $Rb^+$, $Cs^+$, or $NH_4^+$. While the voltage shift phenomenon described in Methods considerably complicates these measurements, definite conclusions can still be drawn. Taking the progressive shift into account and by alternating the bath between Ringer and K-Ringer solution, we were unable to discern any effect on the *g-V* relation of raising external $K^+$ from 4.5 to 160 mM. We therefore use Ringer and K-Ringer solutions interchangeably as reference solutions throughout

this study. In Fig. 2 *A*, when the bath was changed from K-Ringer (■) to $NH_4$-Ringer solution (▲), the *g-V* curve shifted to the *right* by ~15 mV. In view of the spontaneous leftward shifts seen with time, a shift to the right is indicative of an effect of $NH_4^+$. Most cells did not survive long in $NH_4$-Ringer solution, so the reversibility of the shift was not established. In the experiment in Fig. 2 *B*, the bath was changed from Ringer

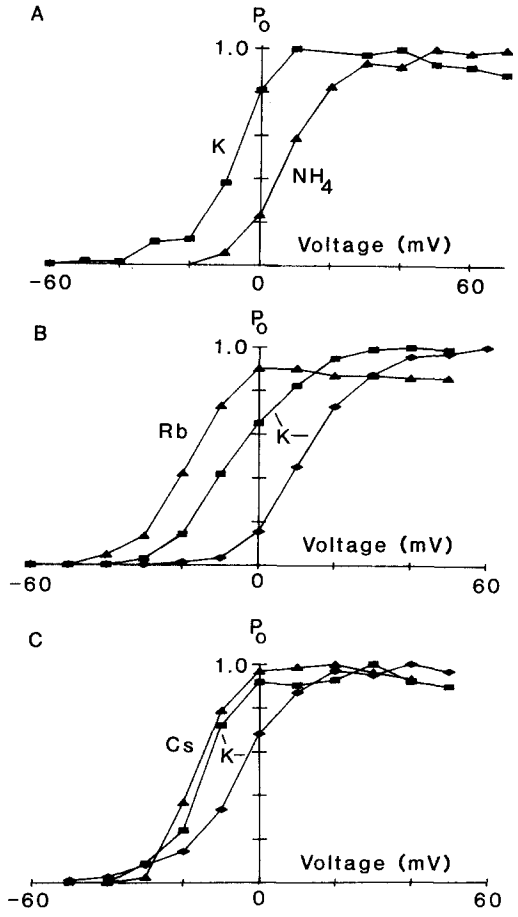


FIGURE 2. Effect of external permeant ion species on the voltage dependence of the type *l* conductance. The normalized peak chord conductance at each potential is plotted, except for the case of $Rb^+$ (▲, *B*), for which the data are the normalized amplitudes of the peak tail transient after each test pulse, extrapolated to zero time after repolarization. For each curve, the half activation potential from a Boltzmann fit to the data and the time in whole-cell are given. (*A*) Effect of $NH_4^+$. The sequence of bath solution was: K-Ringer (■, −6.2 mV, 14 min), and then $NH_4$-Ringer (▲, 10.8 mV, 24 min). Note the small type *n* component around −30 mV evident in K-Ringer solution. Data negative to 0 mV in $NH_4^+$ were lost in the noise. (*B*) Effect of $Rb^+$. Ringer (◆, −4.6 mV, 12 min), Rb-Ringer (▲, −17.6 mV, 27.3 min), and then back to Ringer solution (■, −7.1 mV, 37.4 min). The "droop" in $Rb^+$ at positive potentials is due to a small accumulation of inactivation of the currents during the pulse family applied with an interval of 1 s between pulses (*C*) Effect of $Cs^+$. Ringer (◆, −4.6 mV, 12 min), Cs-Ringer (▲, −16.8 mV, 17 min), and then back to Ringer solution (■, −15.3 mV, 23 min). To calculate each *g-V* curve, $V_{rev}$ was interpolated from the instantaneous *I-V* curves. Pipette: $KCH_3SO_3$ (*A*), $KCH_3SO_3$/F (*B*), KF/Cl (*C*); cell Nos. 31, 78, 106, respectively.

to Rb-Ringer solution, and then back to Ringer. $Rb^+$ shifted the *g-V* curve to the left by ~20 mV, estimated by averaging the pre- and post-Ringer solution controls. Leftward shifts by Rb-Ringer of comparable magnitude were seen in other experiments. A similar experiment performed in a cell with replacement by Cs-Ringer solution is shown in Fig. 2 C. It appears that $Cs^+$ (▲) shifted the *g-V* curve to the left

by a few millivolts compared with pre and post measurements in Ringer solution (◆ and ■, respectively), but the intrinsic voltage shift makes this determination difficult. The effect of $Cs^+$ appears to be less pronounced than that of $Rb^+$, but to the extent that $Cs^+$ may reduce outward currents near threshold potentials, assessing the shift by the peak *g-V* relation may underestimate the effect.

*Macroscopic kinetics.* One of the main observations suggesting occupancy models for other $K^+$ channels is that increasing $[K^+]_o$ slows deactivation (Swenson and Armstrong, 1981; Cahalan et al., 1985; Matteson and Swenson, 1986). In contrast to this result, we saw no effect on $\tau_{tail}$ of raising external $K^+$ from 4.5 to 160 mM. Plotted in Fig. 3 are $\tau_{tail}$ values over a wide potential range for a cell in Ringer solution (◆) and immediately after the bath was changed to K-Ringer solution (■). The two sets of data very nearly superimpose. Similar results were obtained in other experiments in which the order of the solution change was reversed. Throughout the remainder of this paper, we assume that $\tau_{tail}$ in Ringer and in K-Ringer are equivalent and interchangeable as reference solutions for experiments with $K^+$ in the cell. We also saw no effect of $[K^+]_o$ on activation time constants.

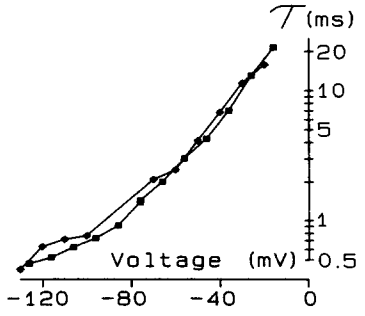


FIGURE 3. Tail time constants in 4.5 (◆) and 160 mM (■) $K^+$ are plotted on semi-logarithmic axes. The two sets of data were obtained in rapid succession. Pipette: $KCH_3SO_3$/EDTA, 16.5°C, cell No. 19.

Replacement of external $K^+$, however, by other permeant ions profoundly affected the rate of deactivation. In Fig. 4, tail current families are plotted for different cells in K-Ringer (*A*), Rb-Ringer (*B*), $NH_4$-Ringer (*C*) and Cs-Ringer solutions (*D*). The tail currents are fast and large in K-Ringer and $NH_4$-Ringer, about half as large and much slower in Rb-Ringer (note the different calibrations), and both slow and very small in amplitude with Cs-Ringer in the bath. Note the expansion of the current scale in the $Cs^+$ family.

The voltage shift phenomenon (Methods) complicated the study of permeant ion effects on kinetics. That the tail current time constant, $\tau_{tail}$, tended to shift less than the time constant of activation, $\tau_{act}$, was favorable since only $\tau_{tail}$ was affected by permeant ion species. All of the conclusions reached on the effects of permeant ions on gating kinetics were confirmed by using a protocol wherein the "test" cation was sandwiched between measurements in a "control" solution such as Ringer or K-Ringer solution.

Activation and deactivation time constants from a cell with K-Ringer and Rb-Ringer solution (ignoring the "hook" for $Rb^+$, companion paper) successively in the

bath are plotted in Fig. 5. Replacing external $K^+$ by $Rb^+$ increased $\tau_{tail}$ by >10-fold. The slowing effect in many experiments was slightly more pronounced at more positive potentials. Activation time constants, on the other hand, were unaffected by $Rb^+$. The $\tau$-$V$ curves for the $K^+$ and $Rb^+$ data are both approximately bell shaped, with activation and deactivation time constants seeming to converge near the peak. The midpoint of the $g$-$V$ relation, $V_{½}$, for the K-Ringer family in this cell was −24 mV;

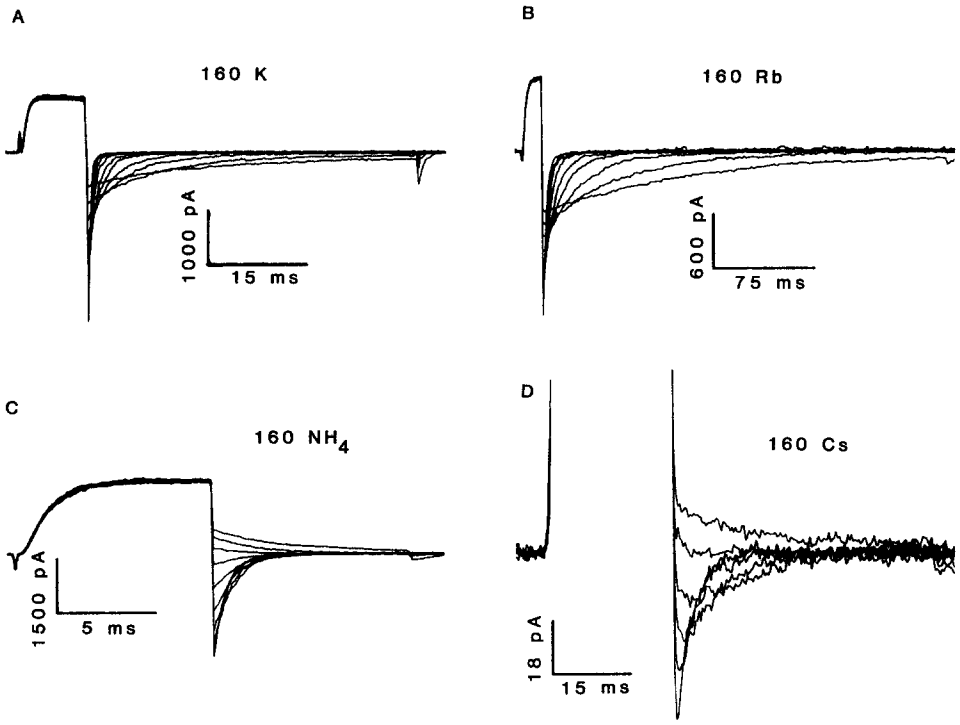


FIGURE 4. Tail currents in the presence of 160 mM of the four permeant ions. Tail currents were collected by applying a brief pre-pulse to 40 mV to open channels maximally and then stepping to various test potentials where deactivation occurs. (*A*) K-Ringer solution. Test pulses from −120 to −20 mV every 10 mV. Filter 2 kHz. (*B*) Rb-Ringer. Test pulses from −120 to −40 mV every 10 mV. Filter 1 kHz. (*C*) $NH_4$-Ringer. Test pulses from −120 to −30 mV every 10 mV. Filter 10 kHz. (*D*) Cs-Ringer. Test pulses to −120, −100, −80, −60, −40, −30 mV. Note the expansion of the current scale. Filter 2 kHz. Series resistance compensation was 80–85% in all except 0% in *D*. Pipette: $KCH_3SO_3$ in all except KF/Cl in *A*. P/4 leak subtraction was used in all except P/8 in B. Cells Nos. 111, 78, 57, 12, respectively.

for Rb-Ringer $V_{½}$ was −44 mV, near the peaks of the $\tau$-$V$ curves for the two ions, respectively.

Fig. 6 shows the voltage-dependence of $\tau_{tail}$ with $K^+$, $Cs^+$, or $NH_4^+$ in the bath. In $Cs^+$ and $NH_4^+$, the currents reverse at −55 mV, partway through the voltage range studied. Negative to $V_{rev}$, the external permeant ion carries the net current, whereas positive to $V_{rev}$, the internal ion (here $K^+$) carries outward currents. For $NH_4^+$, at

negative potentials where there are inward tail currents, $\tau_{tail}$ is about three times slower than its value in K-Ringer solution. At potentials positive to $V_{rev}$, $\tau_{tail}$ is actually slightly faster, qualitatively consistent with the observed 10–15-mV right-shift of the $g$-$V$ curve in $NH_4^+$. The current-dependence of the effect of $NH_4$-Ringer on $\tau_{tail}$ resulted, in this cell, in the $\tau_{tail}$-$V$ relation being nonmonotonic around $V_{rev}$. Deactivation in Cs-Ringer solution was slowed 5–10-fold, even positive to $V_{rev}$, where there are net outward $K^+$ currents. Thus, the effect of $NH_4$-Ringer but not Cs-Ringer solution on $\tau_{tail}$ appears to depend on the direction of current.

The case of $Cs^+$ was indeed quite peculiar. Besides the "hooks" and "washout" phenomena described in the companion paper (Shapiro and DeCoursey, 1991*b*), recovery from inactivation appeared to be slowed profoundly with Cs-Ringer solution in the bath. This conclusion was inferred from experiments in which repetitive depolarizing pulses were applied with a variable interval between pulses. With Ringer solution in the bath, a 2-s interval was sufficient to prevent accumulation of inactivation, even late in the experiment when recovery typically seemed slower. In

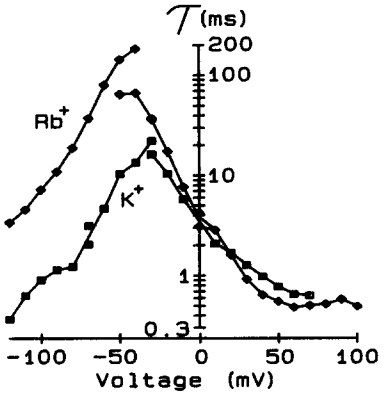


FIGURE 5. Activation (*open symbols*) and deactivation (*filled symbols*) time constants are plotted with K-Ringer (■, □) and Rb-Ringer solution (◆, ◇) successively in the bath. The replacement of external $K^+$ with $Rb^+$ profoundly slows $\tau_{tail}$ but does not affect $\tau_{act}$. Time in whole-cell, 40–55 min; pipette: $KCH_3SO_3$, 19–20°C, cell No. 33.

Cs-Ringer, however, inactivation still accumulated appreciably with 10 s between pulses. Full recovery required a 30-s interval or more. Precise quantification of this effect was difficult since the intrinsic "washout" of the conductance operated also on this time scale. Inactivation seemed somewhat more pronounced also in $NH_4$-Ringer solution.

*Microscopic kinetics.* We studied the closing kinetics of single channel currents with $Rb^+$ in the pipette using on-cell patches. As was discussed for on-cell patch experiments with $K^+$ in the pipette (companion paper), type *n* channels as well as type *l* channels were often encountered in patches, but could be discriminated by their lower unitary conductance (especially with $Rb^+$ as the current carrier). Fig. 7 shows on-cell patch data with a $Ca^{2+}$-free, 160 mM $Rb^+$ pipette solution. Shown in Fig. 7 *A* are three records elicited (as shown) by applying a brief pre-pulse to 0 mV, which opens channels, and then stepping back to −80 mV where channel closing is observed. In the first two records, only one type *l* channel was open at the end of the prepulse, which closes and does not reopen upon repolarization, similar to the case

of $K^+$ in the pipette but with a much longer open time. In the third trace, two type *l* channels were open at the end of the prepulse, and one reopens during the tail pulse. In Fig. 7 *B*, the open time histogram is shown, fit to a single exponential with $\tau$ = 6.6 ms. The ensemble current from this experiment is shown in Fig. 7 *C*, fit to a double exponential, with $\tau_{fast}$ = 10.2 ms and a small slow component with $\tau_{slow}$ = 89.5 ms. The slow component is due to occasional type *n* events (not shown), which were clearly evident in the records. We interpret the 50% longer ensemble vs. histogram time constant (10.2 vs. 6.6 ms) as smearing of the fast component by occasional reopenings, as in the lower record in Fig. 7 *A*. Although reopenings ought to add a small separate slower component to the ensemble, the data are not adequate to resolve three exponentials. Considering the difference in $[Ca^{2+}]_o$ in the two measurements (<43 nM vs. 2 mM) and the intrinsic whole-cell voltage shift (Methods), the ensemble time constant is similar to $\tau_{tail}$ for the whole-cell measurements with Rb-Ringer solution in the bath, and ~13 times slower than the corresponding

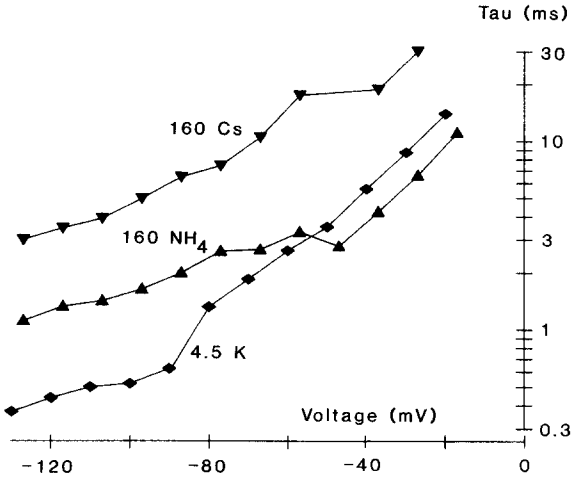


FIGURE 6. Deactivation time constants with Cs-Ringer or $NH_4$-Ringer solution compared with Ringer solution in the bath. After measurements in Ringer (◆), the bath was immediately changed to $NH_4$-Ringer (▲), and finally to Cs-Ringer (▼). Estimated by interpolation of tail current amplitudes (i.e., from the instantaneous *I-V* relation), $V_{rev}$ was −52.4 mV in $NH_4$-Ringer and −52.5 mV in Cs-Ringer solution. Time in whole-cell 7–21 min, 20°C, cell No. 12.

measurement on-cell with $K^+$ in the pipette (companion paper). Thus, as with $K^+$ in the pipette, type *l* channels in on-cell patches close normally in the presence of only nanomolar concentrations of external $Ca^{2+}$. In addition, in both whole-cell and single channel determinations, the slowing of closing kinetics by external $Rb^+$ is similar.

*Currents with $Rb^+$ or $Cs^+$ in the Cell*

All of the data presented so far have been with $K^+$ as the only internal monovalent cation. In experiments described next, the pipette solution contained $Rb^+$ or $Cs^+$ instead of $K^+$. The pipette solution was not changed during a particular experiment. Equilibration of small cations between the pipette and a small cell such as a lymphocyte is reached within seconds after breaking into the cell (Pusch and Neher, 1988) so the identity of the pipette permeant is the same as that in the cell. Fig. 8 illustrates an experiment with RbF/Cl in the pipette. The currents with $Rb^+$ in the cell (Fig. 8 *A*) are very similar to those with intracellular $K^+$, with half-activation for the

*g-V* calculated for this family at −5 mV. When the bath was changed to Rb-Ringer solution, activation was shifted in the negative direction by 23 mV, similar to the effect of Rb-Ringer with $K^+$ in the cell described in Fig. 2 *B*. Plotted in Fig. 8 *B* are values of $\tau_{tail}$ for this cell in Ringer (◆), K-Ringer (■), Rb-Ringer (▲), and Cs-Ringer solution (●). With $Rb^+$ in the cell, the magnitude and voltage dependence of $\tau_{tail}$ for the inward tail currents in K-Ringer, Rb-Ringer, or Cs-Ringer solutions are similar to

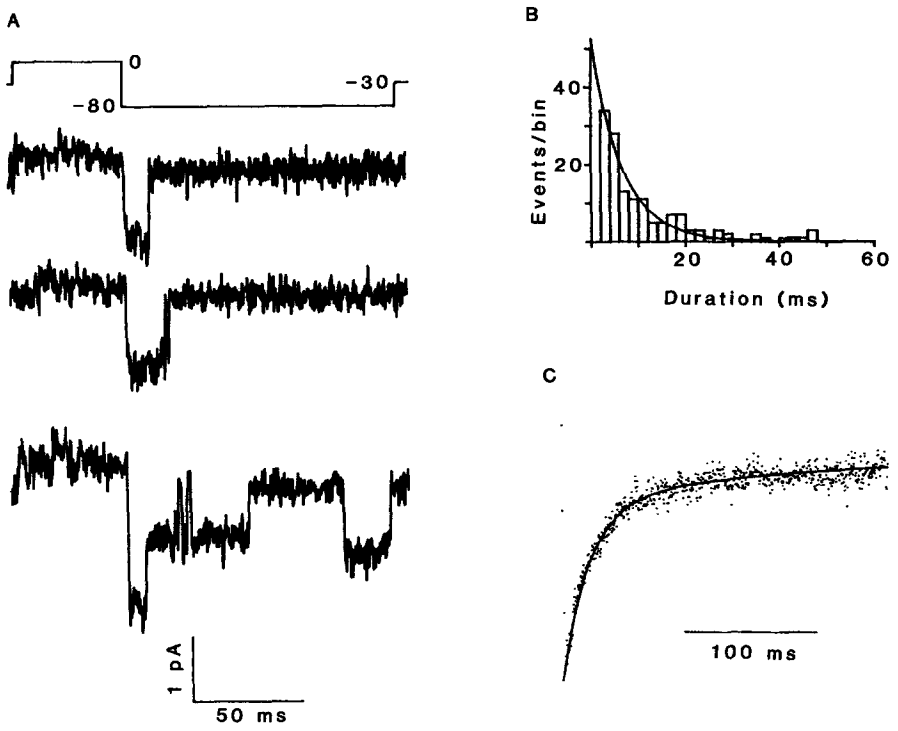


FIGURE 7. On-cell patch with $Rb^+$ in the pipette. (*A*) Three records for the schematic protocol are shown after subtraction of averaged null sweeps. The pre-pulse to 0 mV is very near $V_{rev}$ so little current is evident; open channel currents at −80 mV are inward (downward). Note the clear reopening at −80 mV in the bottom record. The open time histogram from this experiment including only type *l* events is shown (*B*), fit to an exponential by least-squares with $\tau$ = 6.6 ms. The first bin was disregarded in the fit and is not shown. (*C*) The ensemble current for all events, fit to a large fast exponential ($\tau$ = 10.2 ms) and a small slow one ($\tau$ = 89.5 ms). The latter is due to the occasional type *n* channel event in the patch, which stay open much longer than type *l* events. Filter 1 kHz, sample interval 179 μs, pipette RbF/Cl, cell No. 157.

those in each external solution, respectively, in cells with internal $K^+$ (Figs. 5 and 6). Thus, deactivation in K-Ringer is fast and is slowed by about a factor of 10 in Rb-Ringer or Cs-Ringer solution. In Cs-Ringer the tail currents exhibited "hooks" similar to those seen with internal $K^+$. Thus, for the measurements described heretofore, type *l* kinetics seem to depend wholly on the external permeant ion.

The case of Ringer solution in the bath in Fig. 8 *B*, however, is particularly interesting. Here $V_{rev}$ is −80 mV and tail currents negative to that potential are carried by $K^+$ from the bath, and have $\tau_{tail}$ values identical with those in K-Ringer solution. Positive to $V_{rev}$, tail currents are outward and carried by $Rb^+$ from the cell; values for $\tau_{tail}$ diverge from those in K-Ringer at $V_{rev}$ and are increasingly slowed at

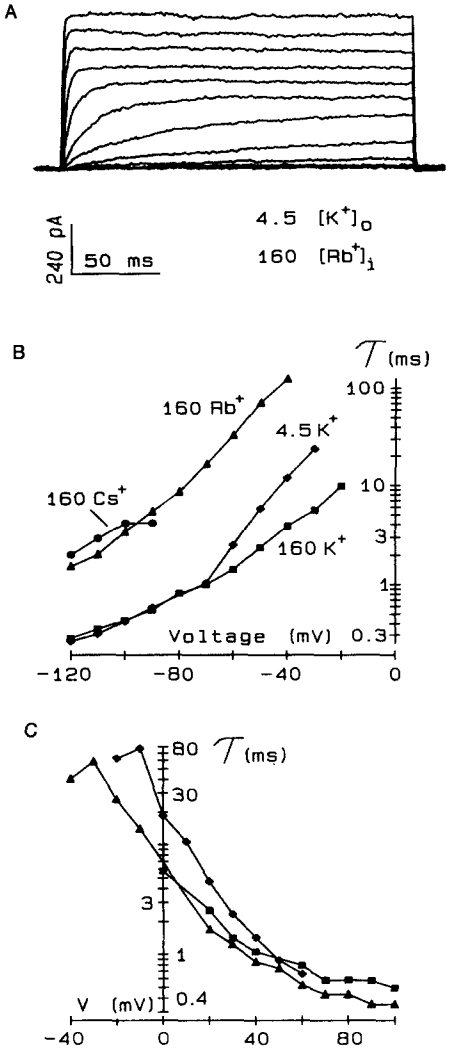


FIGURE 8. Experiments with $Rb^+$ in the cell. (*A*) Family of whole-cell currents with Ringer solution in the bath, during 200-ms pulses to potentials between −60 and 30 mV every 10 mV. *P*/5 leak subtraction, 0% SR, filter 1 kHz. (*B*) Deactivation and (*C*) activation time constants from the cell in *A* with internal $Rb^+$. (*B* and *C*) The bath was initially Ringer solution (◆), then changed to K-Ringer (■), then to Cs-Ringer (●), and finally to Rb-Ringer (▲). For the tail time constants in *B*, all of the tail currents except those positive to $V_{rev}$ in Ringer (−70 mV, *arrow*) are inward and carried by the permeant ion in the bath. In Ringer solution, at potentials positive to −70 mV, tail currents are outward and carried by $Rb^+$ from the cell. Times in whole-cell: Ringer 4 min; K-Ringer, 30 min; Cs-Ringer, 36 min; Rb-Ringer 50 min. Pipette solution RbF/Cl, 24°C, cell No. 49.

more positive potentials, but are still substantially faster than the inward tail currents in Rb-Ringer at the same potentials. This result suggests that the external permeant ion is more important than the internal permeant ion, but that $\tau_{tail}$ is detectably affected in some cases by the ionic species carrying net current.

In Fig. 8 *C*, activation time constants, $\tau_{act}$, are plotted for the same cell with Ringer, K-Ringer, or Rb-Ringer solution in the bath. It was shown in Fig. 5 that $\tau_{act}$ with $K^+$ internally is unaffected by the external $Rb^+$; at most potentials where $\tau_{act}$ is measurable, $K^+$ is the main current carrier. With $Rb^+$ in the cell (Fig. 8 *C*), $Rb^+$ carries outward current at positive potentials and so its effect on activation kinetics can be tested directly. By comparison with data with $K^+$ in the cell, it appears that activation kinetics are essentially independent of whether $K^+$ or $Rb^+$ carries net current. Given the intrinsic voltage shift of $\tau_{act}$, the best demonstration of this result is that data from experiments with $Rb^+$ in the cell shown in Fig. 1 *B*(×) superimpose on data with other internal solutions.

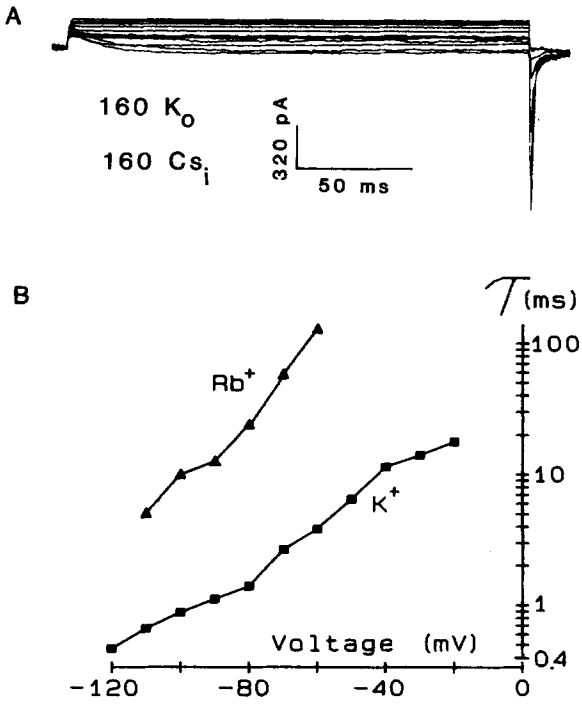


FIGURE 9. Experiment with $Cs^+$ in the cell. (*A*) Superimposed are currents during 200-ms depolarizations to potentials between −40 and 80 mV in 10 mV increments in a cell with CsF/Cl in the pipette and K-Ringer in the bath. No leak subtraction has been used. Note the large, fast inward tail currents. (*B*) Deactivation time constants for the cell in *A* with internal $Cs^+$ and (■) K-Ringer or (▲) Rb-Ringer in the bath. Tail kinetics are indistinguishable from those with $K^+$ in the cell (e.g., Figs. 3 or 5), or with $Rb^+$ in the cell (Fig. 8 B). SR compensation 85%, 18.5°C, filter 1 kHz.

Experiments with $Rb^+$ in the pipette proceeded similarly to those with $K^+$. However, with a $Cs^+$ solution in the pipette, an additional voltage-independent K-selective conductance often appeared (data not shown), interfering with measurements of type *l* $K^+$ currents. This conductance was described previously in *Loucke*s lymphoma cells (A-IR currents; Shapiro and DeCoursey, 1988). In any event, some cells studied with Cs-containing pipette solutions exhibited large type *l* currents that could be identified by their (*a*) voltage-dependence, (*b*) kinetics of activation, (*c*) kinetics of deactivation, and (*d*) sensitivity to block by external $TEA^+$. Currents in a lymphocyte with large type *l* currents but negligible A-IR currents with $Cs^+$ in the pipette and K-Ringer solution in the bath are shown without leak correction in Fig. 9*A*. Depolarization above threshold results in inward type *l* currents over a wide voltage range, with large, fast tail transients upon repolarization. Plotted in Fig. 9 *B*

are values for $\tau_{tail}$ in this cell with internal $Cs^+$ and K-Ringer (■) or Rb-Ringer solution (▲) in the bath. These data are nearly identical to those with internal $K^+$ or $Rb^+$ (Figs. 5, 8 *B*, or 10), with $\tau_{tail}$ in K-Ringer fast and in Rb-Ringer slowed by about an order of magnitude. Thus, the presence of $Cs^+$ in the cell has no obvious effect on the inward $K^+$ or $Rb^+$ tail current kinetics, which in contrast are profoundly slowed by $Cs^+$ in the bath.

### *Current-dependent Permeant Ion Effects*

*Experiments with 10 mM $Rb^+$ in the bath.* Although most of the data presented thus far could be explained by the idea of a modulatory site for $K^+$ channel deactivation that is sensitive to the species of permeant ion in the external solution, the data in Fig. 8 *B* with $Rb^+$ internally and Ringer solution in the bath (◆) seem to indicate that the ion species carrying net current can also modulate deactivation kinetics. To test these ideas further, we studied five cells with $K^+$ in the cell and 5 or 10 mM $Rb^+$ in the bath as the only external permeant ion. Fig. 10 *A* shows the results from a cell with $K^+$ in the pipette and 10 mM $Rb^+$, 150 mM $Li^+$ in the bath. $Li^+$ has no measurable permeability through type *l* channels and does not obviously affect type *l* current kinetics when substituted for $Na^+$ in the bath (data not shown). Plotted are deactivation time constants for Ringer solution in the bath (◆), after the bath was changed to 10 mM $Rb^+$ (×), to 160 mM Rb-Ringer (▲), and then back to Ringer solution (■). At potentials negative to $V_{rev}$ at −64 mV, the inward tail currents (carried by $Rb^+$) in 10 mM $Rb^+$ are as slow as tail currents in Rb-Ringer solution at the same potentials. The outward tail currents (carried by $K^+$), however, are about as fast as the "before" and "after" sets of data points with Ringer solution in the bath. Thus the direction of net current in the presence of 10 mM $Rb^+$ in the bath strongly affects $\tau_{tail}$. A similar dependence on tail current direction of the slowing effect of 5 mM $Rb^+$ was observed in mammalian skeletal muscle (Beam and Donaldson, 1983).

Fig. 10 *B* shows the midpoint of the *g-V* relation, $V_{½}$, measured at various times in each of the solutions studied in this experiment. Only Rb-Ringer solution affects the voltage dependence of $g_K$; the changes in $V_{½}$ in the presence of 10 mM $Rb^+$ are comparable to the shift of $V_{½}$ at different times in Ringer solution (see Methods), consistent with the lack of effect of 10 mM $Rb^+$ on closing kinetics in the voltage range positive to $V_{rev}$.

### *Deactivation Kinetics in Mixtures of $K^+$ and $Rb^+$*

To evaluate the relative effectiveness of $K^+$ and $Rb^+$ in modifying $\tau_{tail}$ in mixtures of the two ions, kinetic measurements were made in various mole fractions of the two, keeping the total permeant ion concentration constant at 160 mM. Fig. 11 summarizes the results of many such experiments. In Fig. 11 *A* the conductance measured 30 mV negative to $V_{rev}$ is plotted. As might be expected if $Rb^+$ ions permeate type *l* channels more slowly than $K^+$ ions and occupy the channel enough to impede $K^+$ permeation, small additions of $Rb^+$ apparently have disproportionate effects on the conductance. The mole fraction dependence of $\tau_{tail}$ plotted in Fig. 11 *B*, however, is surprising. Little slowing of $\tau_{tail}$ is observed until the $Rb^+$ mole fraction is large. This result is consistent with the idea that deactivation kinetics are determined by a modulatory site that is preferentially exposed to the external medium (see Discus-

sion). Superimposed on the data is the theoretical relationship expected from such a modulatory site model, assuming equal affinities for the site of $K^+$ and $Rb^+$.

## DISCUSSION

### *Permeant Ion Effects on the g-V Curve*

The voltage dependence of the *g-V* relation of type *l* $K^+$ channels in lymphocytes varied depending on the species of permeant ion in the external solution. Rb-Ringer

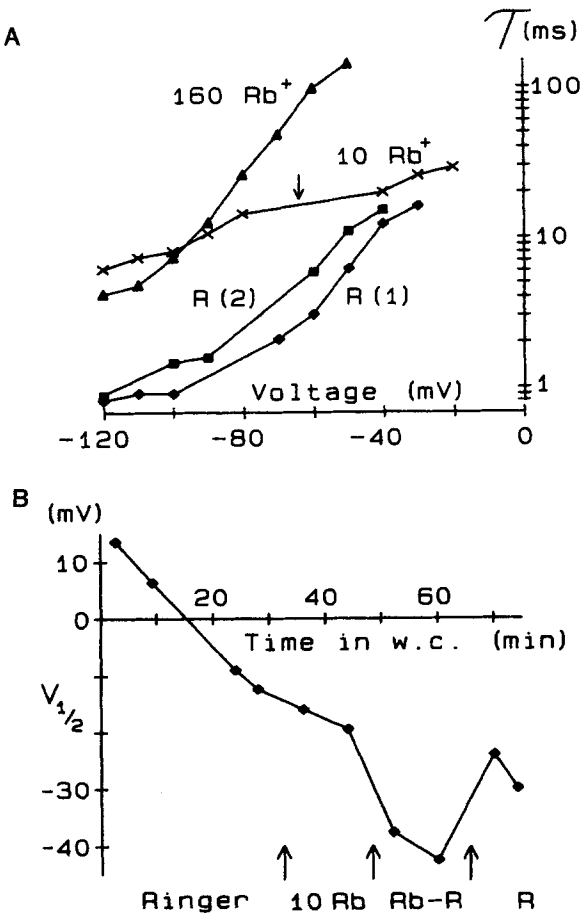


FIGURE 10. (*A*) Tail time constants in a whole-cell (*w.c.*) experiment with 160 $[K^+]_i$. The bath solution was first Ringer (◆), then 10 mM $Rb^+$, 150 mM $Li^+$ (×), then Rb-Ringer (▲), and then Ringer solution, (■). Tail currents negative to $V_{rev}$ in 10 mM $Rb^+$ (*arrow*) are inward $Rb^+$ currents and decay slowly; those positive to $V_{rev}$ are outward $K^+$ currents and are as fast as those in Ringer solution. (*B*) The half-activation potential, $V_{½}$, is plotted at various times in the experiment when the bath contained 4.5 $K^+$ (*Ringer* up to first upward arrow), 10 mM $Rb^+$ (2nd ↑), 160 mM Rb-Ringer (*Rb-R* 3rd ↑) and again Ringer (*R*, after 3rd ↑). Only Rb-Ringer solution shifts the $g_K$ voltage-dependence; the other measurements follow the observed intrinsic $g_K$ voltage shift with time in whole-cell. Times in whole-cell when $\tau_{tail}$ was measured: Ringer (*1*) 26 min; 10 mM $Rb^+$ 40 min; Rb-Ringer 55 min; Ringer (*2*) 70 min. Pipette solution $KCH_3SO_3/F$, 22°C, cell No. 73.

solution in the bath shifted the type *l* *g-V* relation by ~20 mV to more negative potentials; $Cs^+$ produced a smaller negative shift, and $NH_4^+$ shifted the *g-V* relation by ~15 mV to more positive potentials. Qualitatively similar phenomena have been reported for other types of $K^+$ channels: $Rb^+$ produces negative shifts of 10–15 mV in nerve (Cahalan and Pappone, 1983; Plant, 1986; Matteson and Swenson, 1986) and $NH_4^+$ a positive shift of ~10 mV in human lymphocyte type *n* channels (Cahalan et al.,

1985). The effects of permeant ions on the $g$-$V$ relation of type $l$ $K^+$ channels are somewhat more profound than those for other channels.

It seems reasonable to ascribe the effects of permeant ions on the $g$-$V$ relation to their effects on the deactivation rate alone, since activation kinetics were not measurably affected. Approximating type $l$ gating kinetics by a two-state model, if the closing rate is reduced by $Rb^+$ then: (*a*) the $g$-$V$ relation will be shifted to the left, and (*b*) the maximum of the $\tau$-$V$ relation will be larger at $V_{1/2}$. Both effects are observable in the data, and the observed slowing of deactivation accounts quantitatively for both. This interpretation is also supported by the experiment illustrated in Fig. 10 *B*. In

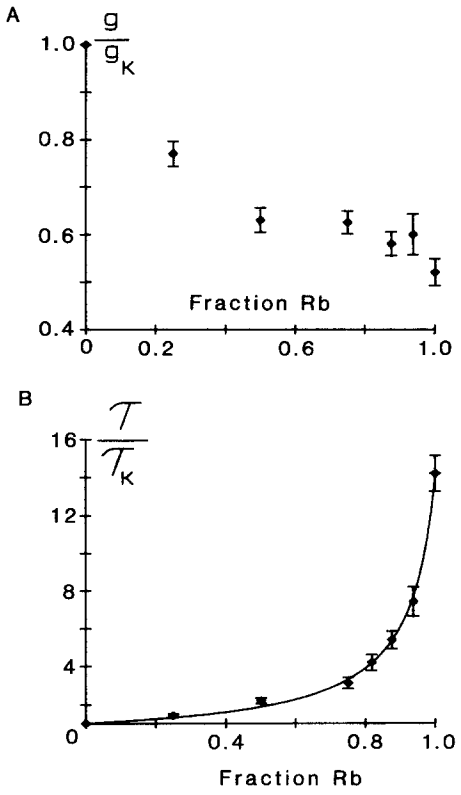


FIGURE 11. $K^+/Rb^+$ mole fraction experiments. (*A*) Dependence of "instantaneous" conductance on mole fraction of $Rb^+$. Mean values of chord conductance ($G_{chord}$) are plotted for each $K^+/Rb^+$ mixture (with $[K^+]_o + [Rb^+]_o = 160$ mM), calculated by taking the extrapolated tail current at $-70$ mV and dividing by the driving voltage in each case. (*B*) Dependence of $\tau_{tail}$ on $Rb^+$ mole fraction. Plotted are mean values for $\tau_{tail}$ at $-70$ mV measured in mixtures of $K^+$ and $Rb^+$. The bars indicate standard errors in both *A* and *B* of 2–10 measurements. Data in both *A* and *B* are normalized to the value ($G_{chord}$ or $\tau_{tail}$) measured at the same potential in the same cell in K-Ringer solution. The curve in *B* shows the mole- fraction dependence assuming the modulatory site model described in the text.

160 mM $Rb^+$, $\tau_{tail}$ was slowed over the whole range within which it could be measured, and the $g$-$V$ curve was shifted. In 10 mM $Rb^+$, $\tau_{tail}$ was slowed negative to $V_{rev}$, but not at more positive potentials, and the $g$-$V$ curve was not shifted. Thus the $g$-$V$ relation depends on the closing rate at potentials around threshold, and not merely on the species of permeant ion in the external solution. The negative shift of the $g$-$V$ in Cs-Ringer solution is at least qualitatively consistent with the slowing of $\tau_{tail}$ by $Cs^+$.

Although $NH_4^+$ slowed $\tau_{tail}$ for inward tail currents negative to $V_{rev}$, it decreased $\tau_{tail}$ at more positive potentials, consistent with the positive shift in the $g$-$V$ relation. Unlike other permeant ions, $NH_4^+$ alters activation kinetics, shifting the $\tau_{act}$-$V$ relation

to more positive potentials. A speculative interpretation of the positive shift of the $g$-$V$ and $\tau$-$V$ curves in $NH_4$-Ringer solution is that the $NH_4^+$ ion protonates a site in or near the channel pore. Gating would then shift to the right, as is observed in experiments with low pH solutions in $Na^+$ (Hille, 1968) and $K^+$ (Hille, 1968; Drouin and The, 1969) channels. Alternatively, $NH_3$ may permeate the membrane and then be protonated, increasing internal pH and so decreasing screening of internal surface charge. If either interpretation is correct, then the slowing of $\tau_{tail}$ negative to $V_{rev}$ by $NH_4^+$ (▲, Fig. 6) is underestimated, since these values also would be shifted to the right.

*Permeant Ion Effects on Deactivation Kinetics*

The 14-fold slowing of deactivation of type *l* currents in lymphocytes when $K^+$ in the bath is replaced by $Rb^+$ is similar to, but more profound than, the effect of external $Rb^+$ on $K^+$ currents in nerve (Århem, 1980; Swenson and Armstrong, 1981; Cahalan and Pappone, 1983; Matteson and Swenson, 1986), muscle (Beam and Donaldson, 1983), and brown fat cells (Lucero and Pappone, 1989) in which tail currents are about twice as slow in $Rb^+$ as in $K^+$. Cahalan et al. (1985) and Plant (1986) reported a fivefold slowing effect of $Rb^+$ in lymphocytes and myelinated nerve, respectively; Spruce et al. (1989) observed a 10-fold slowing of single channel ensembles in skeletal muscle. Most of the slowing effect of $Rb^+$ on type *l* channels is the result of increased mean open time, although there is apparently a small increase in the number of reopenings. The slowing by $Rb^+$ of deactivation of delayed rectifier channels in skeletal muscle (Spruce et al., 1989) and in neuroblastoma cells (Quandt, F.N., personal communication) is due to increases in both mean open time and number of openings per burst. The magnitude of the permeant ion effects on type *l* $K^+$ channel gating led us to reconsider various possible explanations for this phenomenon. We designed several experiments to test whether the species of ion carrying current or if the species of permeant ion present in the external solution was of dominant importance in determining gating kinetics.

*Sidedness of permeant ion effects.* A number of combinations of internal and external ion species were studied. The sum of these data indicates that the permeant ion species in the external solution has a much greater effect on $K^+$ channel gating kinetics than does the internal ion, a conclusion also reached by Plant (1986) for $g_{f2}$ $K^+$ currents in node of Ranvier. Thus, $\tau_{tail}$ was affected in the same way by K-Ringer, Rb-Ringer, or Cs-Ringer solution, regardless of whether the cell contained $K^+$, $Rb^+$, or $Cs^+$. In every case, when tail currents were *inward,* $\tau_{tail}$ was completely determined by the external permeant ion species, and the internal ion had no discernable effect. In Cs-Ringer solution with $[K^+]_i$ = 160 mM, the external ion slows $\tau_{tail}$ for both inward and outward tail currents. *Internal* ion species had detectable effects on $\tau_{tail}$ only when tail currents were *outward:* $[K^+]_o$ = 4.5 and $[Rb^+]_i$ = 160 mM (Fig. 8 *B*), $[Rb^+]_o$ = 10 and $[K^+]_i$ = 160 mM (Fig. 10 *A*), and possibly $[NH_4^+]_o$ = 160 and $[K^+]_i$ = 160 mM (Fig. 6).

These results indicate that the species of external permeant ion has a much greater effect on deactivation kinetics than does the internal ion. If the effects of permeant ions are mediated by a modulatory cation-binding site, the data suggest that this site is located near the external mouth of the type *l* $K^+$ channel, either just within the

permeation pathway or in the external vestibule, but near enough to the pore that outward tail currents significantly alter the local ion concentrations. Dubois and Bergman (1977) proposed that a prerequisite for $K^+$ channel *opening* in myelinated nerve is the binding of a $K^+$ ion to an external site. The site we propose must be functionally distinct from theirs, because permeant ions affect only *de*activation kinetics of type *l* $K^+$ channels.

*Occupancy Models*

The general idea of the "occupancy model" developed for AchR channels (Introduction) was applied by Swenson and Armstrong (1981) to explain the slowing of deactivation in squid delayed rectifier $K^+$ channels by external $Rb^+$ or increased $[K^+]_o$. Beam and Donaldson (1983) interpreted the parallel slowing of $\tau_{tail}$ and reduction of conductance by $Rb^+$ in rat skeletal muscle in terms of an occupancy model. A substantially modified occupancy model has been proposed by Armstrong

TABLE I

*Concentration Dependence of $K^+$ and $Rb^+$ Conductance*

| External ion | $K^+$ in the cell | | |
|---|---|---|---|
| | g | $g_X/g_{X,160}$ | *n* |
| *mM* | *nS* | | |
| 4.5 $K^+$ | 3.56 ± 2.8 | 0.26 ± 0.096 | 13 |
| 160 $K^+$ | 13.9 ± 8.4 | ≡1.0 | 13 |
| 10 $Rb^+$ | 1.70 ± .64 | 0.32 ± 0.024 | 3 |
| 160 $Rb^+$ | 5.21 ± 1.60 | ≡1.0 | 3 |

Conductance values are slope conductances measured at $V_{rev}$-30 mV. In the third column are the mean ± SD of the ratio in each cell of conductances with 4.5 or 10 mM of $K^+$ or $Rb^+$ to that with 160 mM of the same ion. The *n* values are the numbers of cells for which both small and large test concentrations were used in the same cell. The GHK equation predicts conductance ratios at $V_{rev}$-30 mV of 0.06 for $K^+$ and 0.11 for $Rb^+$, assuming $P_{Rb} = 0.76$.

and Matteson (1986) to account also for competition between external $Ca^{2+}$ and permeant monovalent cations, especially $K^+$ and $Rb^+$. In their model, $K^+$ channels can close with either a permeant ion or a $Ca^{2+}$ ion bound within the pore, but the channel "prefers" to close with a $Ca^{2+}$ ion in it; i.e., closing is much faster when the channel is occupied by $Ca^{2+}$ than by a permeant ion. We did not apply this model to the present data because three fundamental observations that led to this model appear not to apply to type *l* $K^+$ channels.

*(a) Conductance and occupancy.* Table I summarizes the conductance data for different concentrations of $K^+$ and $Rb^+$. Increasing $[K^+]_o$ from 4.5 to 160 mM increases the conductance fourfold. This increase is much less than predicted by the GHK independence relation, suggesting that significant interaction between permeating $K^+$ ions occurs; i.e., that the type *l* channel is occupied significantly in 160 mM $K^+$. Nevertheless, four times as many $K^+$ ions permeate the pore per unit time for a given driving force, so the occupancy of any particular site within the channel must

increase appreciably when $[K^+]_0$ is increased from 4.5 to 160 mM, unless the site is essentially always occupied regardless of $[K^+]_o$. Similarly, the conductance increases threefold when $[Rb^+]_o$ is increased from 10 to 160 mM (Table I), which is less than predicted by the GHK model, suggesting interaction between $Rb^+$ ions, but also that channel occupancy increases when $[Rb^+]_o$ is increased as well.

The decrease in the closing rate (1.5–2-fold) of $K^+$ channels in several preparations upon elevation of external $K^+$ (Swenson and Armstrong, 1981; Cahalan et al., 1985; Matteson and Swenson, 1986; Lucero and Pappone, 1989) is consistent with an occupancy hypothesis, since the increase in occupancy with higher $[K^+]_o$ should result in slower time constants. In contrast, for inward type *l* tail currents, $\tau_{tail}$ was the same whether $[K^+]_o$ was 4.5 mM or 160 mM, and was similarly unaffected when $[Rb^+]_o$ was increased from 10 mM to 160 mM. It is difficult to account for these results for both $K^+$ and $Rb^+$ using an occupancy model, especially since any such model must assign substantially different values for the affinity of $K^+$ and $Rb^+$ for the modulatory site to account for the slowing effect of $Rb^+$ (see below).

*(b) Effect of $Ca^{2+}$.* Removing $Ca^{2+}$ from the solution surrounding squid axon appears to prevent $K^+$ channel closing, consistent with the idea that occupancy of a $K^+$ channel by $Ca^{2+}$ is a prerequisite for normal channel closing (Armstrong and Lopez-Barneo, 1987). In murine lymphocytes, however, in cell-attached patches with $Ca^{2+}$-free (<43 nM) pipette solutions, single type *l* channels open and close with voltage dependence and kinetics roughly similar to those of macroscopic currents in the whole-cell configuration with 2 mM $Ca^{2+}$ in the external solution. (Lymphocytes in the whole-cell configuration did not survive $Ca^{2+}$-free bath solutions.) This result does not suggest an obligatory role for external $Ca^{2+}$ in type *l* channel gating.

*(c) Permeant ion species.* The relationship between effects of permeant ion species on conductance and on $\tau_{tail}$ is not consistent with a simple occupancy-type mechanism: (*i*) Rb-Ringer solution slows $\tau_{tail}$ 14-fold compared with K-Ringer but reduces the conductance only by one-half, (*ii*) $Rb^+$ and $Cs^+$ slow $\tau_{tail}$ about equally but have radically different conductances, (*iii*) $NH_4^+$ conducts more current than $K^+$ (for a given driving force) but slows $\tau_{tail}$ compared with $K^+$, and (*iv*) Cs-Ringer solution in the bath slows $\tau_{tail}$ both for inward ($Cs^+$) and outward ($K^+$) currents by about the same amount. In summary, there are enough differences between the permeant ion effects on type *l* $K^+$ channels and on $K^+$ channels in other preparations to necessitate a different kind of model.

### *Is an "Occupancy Hypothesis" Consistent with Our Data?*

Even though points *a* and *c* above seemingly make the type *l* channel a poor candidate for an occupancy model, we considered whether the behavior of type *l* $K^+$ channels is consistent with the idea that they cannot close when occupied by a permeant ion. Like other $K^+$ channels (Hille and Schwarz, 1978), type *l* channels apparently have multiple sites in their permeation pathway that can be occupied during permeation (Shapiro and DeCoursey, 1991*b*). In principle, one could propose that any given site (or set of sites) might impede channel closing when occupied by a permeant ion (or ions). For the purpose of this discussion we consider simply the idea that one site in the permeation pathway prevents closing in an all-or-none manner when occupied by a permeant ion.

*Occupancy in a one-site channel.* We first consider a simple one-site channel (e.g., Marchais and Marty, 1979). We assume that the entry rates for $K^+$ and $Rb^+$ are the same since $P_{Rb}$ is similar to $P_K$ and that the closing rate ($\beta$) at a given potential is directly proportional to the fraction of time the site is *not* occupied, so $\tau_{tail} \sim 1/\beta \propto 1/[1 - \text{occupancy}]$. Since $\tau_{Rb}/\tau_K \sim 14$, the fraction of time the channel/site is *not* occupied must be 14 times greater in $K^+$ than in $Rb^+$. This could be achieved at various absolute occupancies, so we consider two extreme cases. In the high occupancy case the channel is occupied 98.6% of the time in $K^+$ and 99.9% of the time in $Rb^+$ (i.e., unoccupied 1.4 or 0.1% of the time, respectively), and the site must have a 14.2-fold greater affinity for $Rb^+$ than for $K^+$. In this high occupancy case, when either $[K^+]_o$ or $[Rb^+]_o$ are altered, [1−occupancy] and consequently $\tau_{tail}$ must significantly change. In the low occupancy case the same 14-fold difference in [1−occupancy] could also be achieved if the channel were occupied negligibly in $K^+$ and 93% of the time in $Rb^+$, in which case the relative affinity of the site for $Rb^+$ is infinitely greater than that for $K^+$. Now there would be no detectable change in $\tau_{tail}$ when $[K^+]_o$ is increased from 4.5 to 160 mM, but still a pronounced effect in raising $[Rb^+]_o$ from 5 or 10 to 160 mM, in contrast with the data.

In mixtures of $K^+$ and $Rb^+$, $\tau_{tail}$ was not much slowed until the $Rb^+$ mole fraction was large (Fig. 11 *B*); i.e., the relationship between $Rb^+$ mole fraction and $\tau_{tail}$ was strongly concave. In a one-site channel with an occupancy-type mechanism and equal entry rates for $K^+$ and $Rb^+$, regardless of absolute occupancy of the channel, there is a linear relationship between $Rb^+$ mole fraction and $\tau_{tail}$. Even if $Rb^+$ is assigned a lower entry rate than $K^+$, as might be expected from the lower $P_{rel}$ and $g_{rel}$, the calculated $\tau_{tail}$ vs. $Rb^+$ mole fraction relationship remains linear. In conclusion, a simple occupancy model in a one-site channel does not fit our data.

*Occupancy in an Eyring model.* Matteson and Swenson (1986) used a two-site, three-barrier Eyring model to simulate the permeation and selectivity of $K^+$ channels in squid. They found that occupancy of the inner site by monovalent cations in their model was correlated with slowing of the $\tau_{tail}$; that is, both occupancy and $\tau_{tail}$ were increased by increasing $[K^+]_o$ or by replacement of external $K^+$ by $Cs^+$ or $Rb^+$, and both were decreased by replacing external $K^+$ by $Tl^+$ or $NH_4^+$. Since we do not have a large enough body of data to constrain the parameters of even a two-site Eyring model adequately, we have explored this type of model with a nonexhaustive sample of more or less arbitrarily chosen parameters.

If the $K^+$ channel can close only when the inner site is *not* occupied by either $K^+$ or $Rb^+$, then $\tau_{tail}$ is proportional to the inverse of the probability that the inner site is empty. Starting with barrier heights and well depths and positions used by Matteson and Swenson (1986) for $K^+$ and $Rb^+$ in squid, we made the inner well for $Rb^+$ deeper by −1.8 RT units to increase the calculated $\tau_{tail}$ ratio to 14 for Rb-Ringer vs. K-Ringer solution, resulting in high inner site occupancy for both K-Ringer (0.797) and Rb-Ringer (0.986). The calculated $\tau_{tail}$ increased rapidly with increasing $Rb^+$ mole fraction, with a convex dependence on the mole fraction, in sharp contrast to the observed relationship in Fig. 11 *B*. Varying the well positions had little effect on this relationship. The greater well depth for $Rb^+$ results in substantial occupancy of the site by $Rb^+$ for even small additions to the external solution. In general, a site within the permeation pathway that is occupied longer by $Rb^+$ than by $K^+$ during

permeation (i.e., with a higher affinity for $Rb^+$) will be occupied disproportionately by $Rb^+$ in mixtures with $K^+$ and so a concave mole fraction relationship is not to be expected. Using several other sets of Eyring parameters selected to approximate more closely the observed *I-V*s in $Rb^+$ and $K^+$ solutions, the $Rb^+$ mole fraction dependence of $\tau_{tail}$ was either convex or roughly linear. Assuming that occupancy of the outer site rather than the inner site determines $\tau_{tail}$ gave similar results, but usually with less pronounced convexity.

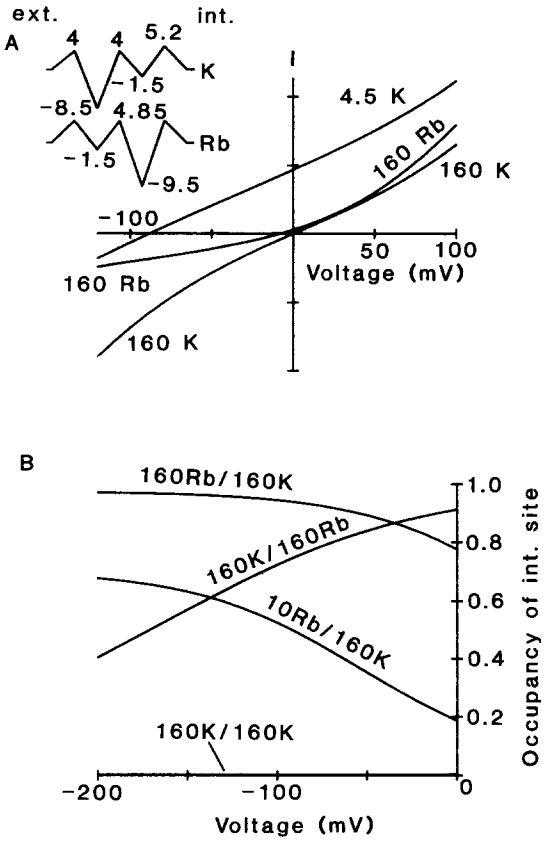


FIGURE 12. (*A*) Current-voltage relationships calculated with a three-barrier, two-site Eyring model (see Methods), with parameter values given in the inset in RT units, and equal well spacings. The external permeant ion concentration is indicated near each curve, in each case with 160 mM $[K^+]_i$. The parameter values were chosen to simulate the concave relationship between $\tau_{tail}$ and $Rb^+$ mole fraction shown in Fig. 11 *B*, assuming that inner site occupancy prevents channel closing in an all-or-none manner, with the ratio of time the site is *un*occupied differing by 14.2 between $K^+$ and $Rb^+$. (*B*) Occupancy of the inner site in the channel calculated for the same parameters as in part *A*, with ionic conditions indicated as [external]/[internal] (mM) for the cases of 160 $K^+$/160 $K^+$, 160 $Rb^+$/160 $K^+$, 10 $Rb^+$/160 $K^+$, and 160 $K^+$/160 $Rb^+$. Occupancy is so low for 160 $K^+$/160$K^+$ that the curve is nearly indistinguishable from the abscissa. Note that occupancy increases substantially when $[Rb^+]_o$ is increased from 10 to 160 mM, and that with 160 $[Rb^+]_i$, occupancy is high at all potentials.

Since Eyring parameters chosen in the usual way to imitate instantaneous *I-V* relations seemed not to generate naturally the observed strongly concave dependence of $\tau_{tail}$ on $Rb^+$ mole fraction, we decided simply to adjust the parameters arbitrarily, constrained only to give a reasonable $V_{rev}$ in Rb-Ringer solution. Parameters for $K^+$ and $Rb^+$ were assumed to be concentration independent, and identical barrier and well positions and "frequency factors" were assumed for $K^+$ and $Rb^+$. Values were found (see Fig. 12 *A*, *inset*) that gave a concave $Rb^+$ mole fraction

dependence of $\tau_{tail}$ qualitatively like that observed. These values indicate strong preferential binding of $K^+$ at the outer site and of $Rb^+$ at the inner site. Instantaneous *I-V*s in Fig. 12 *A* calculated using these parameters deviate from real data: there is outward rectification at positive potentials in K-Ringer and in Rb-Ringer solution, the currents are too large in Ringer, and inward currents in Rb-Ringer are too small.

A more significant difficulty with this model is illustrated in Fig. 12 *B*, in which the occupancy of the inner site under various ionic conditions is plotted. Changes in ionic conditions that in real currents do not affect $\tau_{tail}$ have large effects in the model: the calculated $\tau_{tail}$ at −70 mV increases sevenfold when $[Rb^+]_o$ is increased from 10 to 160 mM, and is much slower (greater than fivefold) when internal $K^+$ is replaced by $Rb^+$ with either K-Ringer or Rb-Ringer solution in the bath, indicating high occupancy by $Rb^+$ at all potentials with $Rb^+$ in the cell. Under bi-ionic conditions an ion species with a deeper well can have a greater occupancy at a given site in the channel than the ionic species carrying net current from the other side of the membrane. This phenomenon is an important consideration in light of the complete lack of detectable effect of internal $Rb^+$ or $Cs^+$ on $\tau_{tail}$ for inward currents, and the sharp dependence on current direction of the $\tau_{tail}$ data with 160 $[Rb^+]_i$ and Ringer solution in the bath, or with 160 $[K^+]_i$ and 10 $[Rb^+]_o$ (see above).

In summary, although we have not been able to find any set of Eyring parameters that can account for all the data using an occupancy model, we cannot rule out the possibility that such parameters might exist, especially if more sites were added to the model. However, it seems very difficult *simultaneously* to account for (*a*) the slight or negligible effect of the internal ion species on $\tau_{tail}$, (*b*) the lack of effect of increasing $[K^+]_o$ from 4.5 mM to 160 mM or of increasing $[Rb^+]_o$ from 5 or 10 mM to 160 mM, (*c*) the concave $Rb^+$ mole fraction dependence of $\tau_{tail}$, and (*d*) the similarity of $g_{Rb}$ and $g_K$ given a 14-fold difference in $\tau_{tail}$.

*Voltage and current dependence of $\tau_{tail}$.* One striking feature of the 10 mM $Rb^+$ data in Fig. 10 *A* is the narrow voltage range within which $\tau_{tail}$ switches from $K^+$ to $Rb^+$ (fast to slow) kinetics. When the Ringer solution data in Fig. 8 *B* are expressed in terms of apparent mole fraction $Rb^+$ (see below), a similar steep voltage dependence is observed. In calculations using several sets of Eyring parameters in these two ionic conditions, occupancy of either site in the channel (either by $Rb^+$ or by any permeant ion) varies much less with potential or with the direction of net current than could account for the apparent dependence on current direction of $\tau_{tail}$ that we observed. For example, Fig. 12 *B* shows that for 10 mM $[Rb^+]_o$ and 160 mM $[K^+]_i$, occupancy of the inner site decreases with depolarization, qualitatively as is necessary to produce slow inward and fast outward tail currents (Fig. 10 *A*). However, the voltage dependence is much too shallow. The situation is analogous to simulations of voltage dependent block by a partially permeant ion. Using a two-site Eyring model, French and Shoukimas (1985) found that the steepness of the voltage dependence of block by a moderately permeant blocking ion was more gradual (smaller effective valence) than for a completely impermeant blocking ion. For type *l* channels, $Rb^+$ must be considered a fairly permeant blocker. If one were to postulate a pore with *many* binding sites, it might be possible to quantitatively account for the steepness of the current and voltage dependence of the $\tau_{tail}$ data. However, the problems discussed in the last section remain.

*External Modulatory Site*

An alternative type of model involves a site that modulates the closing rate depending on the species of permeant ion bound to the site. We make three main assumptions: (*a*) Occupancy of a site by $Rb^+$ slows $\tau_{tail}$ by a factor of 14.2 (the mean value of $\tau_{tail}$ in Rb-Ringer compared with that in K-Ringer solution); (*b*) since increasing $[K^+]_o$ or $[Rb^+]_o$ does not detectably alter $\tau_{tail}$ for inward currents, we propose that the modulatory site is essentially always occupied by a permeant ion under these conditions; and (*c*) as a first approximation we assume that $K^+$ and $Rb^+$ have the same affinity for the site, so the fractional occupancy by each cation is directly proportional to its mole fraction in the bath. This model gives the predicted $\tau_{tail}$ vs. $Rb^+$ mole fraction relationship shown in Fig. 11 *B* as a solid line, which is drawn according to: $\tau_{tail} = 1/(f_{Rb}\,\beta_{Rb} + f_K\,\beta_K)$, where $f_{Rb}$ and $f_K$ are the mole fractions of $Rb^+$ and $K^+$, respectively, and $\beta_{Rb}$ and $\beta_K$ are the closing rate constants when the site is occupied by $Rb^+$ or $K^+$, respectively, i.e., $(14.2)^{-1}$ and 1. The agreement of this simple model with the data is remarkable. While any or all of the assumptions might be incorrect, altering any of them would necessitate corresponding alterations in the others in order to maintain the excellent fit to the data. This model does not make any specific prediction about the relative conductance because the site is located outside the single-file region of the pore. $Na^+$ and $Li^+$ apparently either cannot reach the site or have a much lower affinity for the site than do permeant ions, because $\tau_{tail}$ is the same in 4.5 mM $K^+$ (and 160 mM $Na^+$) as in 160 mM $K^+$, and in 5 or 10 mM $Rb^+$ (with 160 mM $Na^+$ or $Li^+$) as in 160 mM $Rb^+$. $Cs^+$ apparently has a greater affinity for the site than does $NH_4^+$ because in Cs-Ringer solution, outward tail currents are slowed dramatically, while in $NH_4$-Ringer outward tails are fast.

*Vestibule site.* The fit of the modulatory site model to the data in Fig. 11 *B* is consistent with an external location for the site, since it apparently is occupied by $K^+$ and $Rb^+$ in direct proportion to their mole fraction in the bath. The detectable effects of the ion species carrying outward current on $\tau_{tail}$ (Figs. 8 *B*, 10, and possibly the $NH_4^+$ effect in Fig. 6; see above: *Sidedness of permeant ion effects*) rule out an external location distant from the pore; the site must be near enough to the outer mouth of the pore that the local ion concentrations are significantly altered by outward tail currents. When there is outward current the modulatory site in the outer antechamber or vestibule apparently "sees" a mixture of the bath solution and the ionic species carrying outward current. In considering such a possibility, the first question is whether it is reasonable to expect that outward current through a single channel could alter local ion concentrations sufficiently to produce the effects observed. We ascribe the slowing of $\tau_{tail}$ positive to $V_{rev}$ with 4.5 mM $K^+$ externally and 160 mM $Rb^+$ internally (◆, Fig. 8 *B*) to local accumulation of $Rb^+$ at the modulatory site. Assuming that the slowing effect is dependent on the mole fraction of $Rb^+$ and not on absolute concentration, we can estimate the local $[Rb^+]$ necessary to produce this slowing using the theoretical relationship plotted in Fig. 11 *B*. In the cell illustrated in Fig. 8 *B*, the apparent $Rb^+$ mole fraction is 0.1 at −70 mV and increases progressively with depolarization to 0.4 at −60 mV and 0.75 at −40 mV. These values correspond to local $[Rb^+]$ of 0.4, 3.1, and 12.4 mM, respectively, estimated after correcting for a slight reduction of $[K^+]$ due to displacement by $[Rb^+]$. In two other experiments

analyzed in this way similar results were obtained: the apparent local $Rb^+$ mole fraction increased rapidly at potentials positive to $V_{rev}$ to >0.8 at 30 mV, corresponding to absolute local [$Rb^+$] approaching 20 mM.

The problem of local ion accumulation and depletion due to current flow through a single ion channel has been considered for the case of a cylindrical channel opening directly into a planar membrane/bath interface (Läuger, 1976). For example, for a 2-pA current, the concentration change is ~10 mM at the effective capture radius ($r_o$, the radius of the mouth of the channel minus the radius of the ion) of a channel with

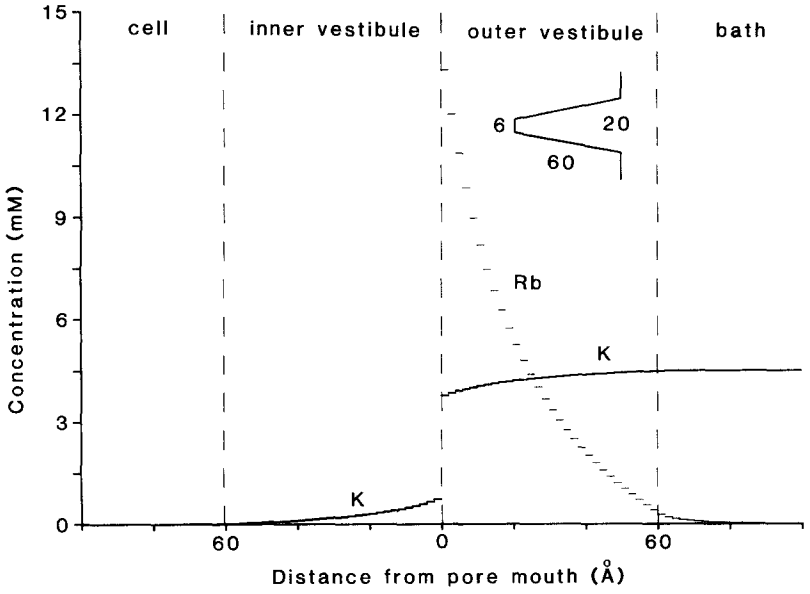


FIGURE 13. Calculated local concentrations of $K^+$ and $Rb^+$ in the vestibules of a hypothetical type *l* $K^+$ channel during a single channel current at −40 mV with 4.5 mM [$K^+$]$_o$ and 160 mM [$Rb^+$]$_i$. The model is described in detail in Methods. Identical vestibules are assumed at each end of the single file region of the type *l* $K^+$ channel, with dimensions indicated in the inset (in Å). Distances are relative to the respective end of the pore (the dimensions of which are irrelevant in these calculations), with the vestibule openings indicated by dashed vertical lines. The component currents are 0.54 pA from the cell to the bath and −0.095 pA for bath-to-cell current, which combine to give a net current of 0.445 pA, corresponding to a conductance of 10 pS. The concentration profile shown is after equilibration which takes ~40 ns.

a 1 Å $r_o$, but falls off rapidly with distance or for larger $r_o$ (Barry and Diamond, 1984). However, if the channel has an outer vestibule, then the ion species carrying outward current would accumulate to a greater extent and the fall-off in concentration with distance would be more gradual.

*Model of vestibular modulatory site.* To test more quantitatively the feasibility of a vestibular location of the modulatory site, we used a simplified diffusion model, illustrated in Fig. 13. We assume an identical vestibule of arbitrary dimensions (as shown), at both ends of the channel pore. Calculations with no inner vestibule gave

generally similar results. Diffusion is driven by current through the channel, which is derived from component unidirectional currents calculated with the GHK current equation, and assuming a unitary conductance of 10 pS. Calculations assuming a flux ratio exponent of 2.5, as found in squid axon $K^+$ channels (Hodgkin and Keynes, 1955; Begenisich and De Weer, 1980) gave quantitatively similar $Rb^+$ accumulation in the outer vestibule, but somewhat steeper voltage dependence. Both the outward and inward current are assumed to be carried in direct proportion to the local relative concentrations of $K^+$ and $Rb^+$, i.e., in the compartments adjacent to the pore, with $[Rb^+]$ scaled by 0.76 to account for its lower permeability. Thus, as $Rb^+$ accumulates in the outer vestibule it contributes to the inward current component.

Fig. 13 illustrates the results of a calculation simulating the local accumulation of ions during an outward tail current at −40 mV in 4.5 mM $K^+$ with 160 mM $Rb^+$ internally (i.e., Fig. 8 *B*). The outer vestibule is divided into 30 compartments, each 2 Å thick. The accumulation of $Rb^+$ is substantial, 13.3 mM in the first compartment, with $[K^+]$ reduced to 3.77 mM due to the inward component of current, corresponding to a $Rb^+$ mole fraction of 0.80. The $Rb^+$ mole fraction falls to 0.69 at 10 Å from the pore mouth, and to 0.5, 26 Å away. In the experiment in Fig. 8 *B*, $\tau_{tail}$ for the outward tail current at −40 mV in Ringer solution was 3.1 times slower than the inward tail current in K-Ringer solution at −40 mV. Interpolating from the theoretical curve in Fig. 11 *B*, this relative $\tau_{tail}$ is equivalent to a $Rb^+$ mole fraction of 0.73, which is comparable to calculated values in the first 10 Å of the outer vestibule. In spite of the many uncertainties involved, it seems that the slowing of $\tau_{tail}$ positive to $V_{rev}$ under these ionic conditions can quantitatively be ascribed to local accumulation of $Rb^+$.

Analogous calculations were done for the case of 10 mM $Rb^+$ in the bath and 160 mM $K^+$ internally (compare Fig. 10 *A*). During calculated outward tail currents, sufficient $K^+$ accumulated in the outer vestibule to lower $\tau_{tail}$ to near its value in K-Ringer solution. The more dramatic effect of outward $K^+$ current on $\tau_{tail}$ compared with the more subtle effect of outward $Rb^+$ current can be explained by the mole-fraction relationship shown in Fig. 11 *B*. In the former case, a small accumulation of $K^+$ would lower the $Rb^+$ mole fraction, greatly reducing $\tau_{tail}$, because the curve is very steep at the high [Rb] end. Accumulation of a comparable mole fraction of $Rb^+$ in the latter case would have a less pronounced effect, because $\tau_{tail}$ is not much affected until the $Rb^+$ mole fraction becomes large. In both of these situations in which the outward current carrier affects $\tau_{tail}$, the permeant ion concentration in the bath is low, so that addition of a few millimolar permeant ion from the cell has a substantial effect on the local mole fraction.

*Limitations of the model and apologetics.* Clearly this model is oversimplified in many respects. (*a*) We do not know the actual inward and outward current fluxes; if the local concentration changes proposed here take place to any extent, then they essentially preclude using any simple model (GHK, Eyring, etc.) to calculate the component ion fluxes because the concentrations at the mouths of the channels are different from the bulk concentrations and depend on current magnitudes. (*b*) We do not know that the modulation of $\tau_{tail}$ is strictly mole fraction dependent, and concentration independent (i.e., that $\tau_{tail}$ is the same in 4 mM $Rb^+$, 4 mM $K^+$ as in 80 mM $Rb^+$, 80 mM $K^+$). The similarity of $\tau_{tail}$ in low and high concentrations of either

$K^+$ or $Rb^+$ supports this assumption but does not prove it. (*c*) We consider only diffusional effects, and neglect the voltage drop due to ion depletion/concentration such as has been detected experimentally by Yellen (1984) for $Ca^{2+}$-activated $K^+$ channels. However, type *l* channels, especially under the ionic conditions in which we observe effects attributable to local permeant ion accumulation, carry much smaller currents than do $Ca^{2+}$-activated $K^+$ channels. Furthermore, Läuger (1976) has shown that when there is a large concentration of impermeant co-ion, as in the present case with 4.5 mM $K^+$ permeant and 160 mM $Na^+$ impermeant, or with 10 mM $Rb^+$ permeant and 150 mM $Li^+$ impermeant, the diffusional gradient becomes much more important than the electrical potential gradient. (*d*) We do not consider the consequences of interactions between ions and the vestibule walls (as in Dani, 1986). The binding of a permeant ion to a vestibular modulatory site, as proposed here, would itself be an example of such an interaction. (*e*) Similarly, we do not consider possible effects of fixed charges in the vestibule on local ion concentrations. Anderson (1983) proposed the existence of fixed negative charges in the antechamber of $K^+$ or $Na^+$ channels as a means of enhancing their unitary conductance. Jordan (1987) has calculated that a single fixed negative charge near the channel mouth can increase local cation concentrations dramatically (1.8-fold or more, depending on the geometry involved), accounting for the large conductance of $Na^+$ channels at very low concentrations (Cai and Jordan, 1990). For the vestibule dimensions and the single channel conductance in our calculations (Fig. 13), $[K^+]$ in the outer vestibule is completely depleted at large negative potentials. This result suggests that fixed negative charges in the type *l* vestibule may be required, although it could also be argued that our choice of vestibule dimensions or other assumptions are incorrect. In conclusion, in spite of uncertainties and simplifying assumptions involved, calculations with this model support the idea that the large concentration changes required to account for our data can occur at a site within the outer vestibule of the type *l* $K^+$ channel.

We thank Dr. Fred N. Quandt for reading and commenting upon this manuscript.

This work was supported by research grant HL-37500 (T. DeCoursey), Research Career Development Award K04-1928 (T. DeCoursey), and by National Research Service Award pre-doctoral training grant HL-07320 (M. Shapiro), all from the National Institutes of Health.

The work presented here was part of that submitted by M. Shapiro in partial fulfillment of the degree of Ph.D.

*Original version received 8 June 1990 and accepted version received 3 December 1990.*

## REFERENCES

Adams, D. J., W. Nonner, T. M. Dwyer, and B. Hille. 1981. Block of endplate channels by permeant cations in frog skeletal muscle. *Journal of General Physiology.* 78:593–615.

Århem, P. 1980. Effects of rubidium, caesium, strontium, barium and lanthanum on ionic currents in myelinated nerve fibres from *Xenopus laevis*. *Acta Physiologica Scandinavica.* 108:7–16.

Anderson, O. S. 1983. Ion movement through gramicidin A channels: studies on the diffusion-controlled association step. *Biophysical Journal.* 41:147–165.

Armstrong, C. M., and J. Lopez-Barneo. 1987. External calcium ions are required for potassium channel gating in squid neurons. *Science.* 236:712–714.

Armstrong, C. M., and D. R. Matteson. 1986. The role of calcium ions in the closing of K channels. *Journal of General Physiology.* 87:817–832.

Ascher, P., A. Marty, and T.O. Neild. 1978. Life time and elementary conductance of the channels mediating the excitatory effects of acetylcholine in *Aplysia* neurones. *Journal of Physiology.* 278:177–206.

Barry, P. H., and J. M. Diamond. 1984. Effects of unstirred layers on membrane phenomena. *Physiological Reviews.* 64:763–872.

Beam, K. G., and P. L. Donaldson. 1983. Slow components of potassium tail currents in rat skeletal muscle. *Journal of General Physiology.* 81:513–530.

Begenisich, T. B., and P. De Weer. 1980. Potassium flux ratio in voltage-clamped squid giant axons. *Journal of General Physiology.* 76:83–98.

Cahalan, M. D., K. G. Chandy, T. E. DeCoursey, and S. Gupta. 1985. A voltage-gated potassium channel in human T lymphocytes. *Journal of Physiology.* 358:197–237.

Cahalan, M. D., and P. A. Pappone. 1983. Chemical modification of potassium channel gating in frog myelinated nerve by trinitrobenzene sulphonic acid. *Journal of Physiology.* 342:119–143.

Cai, M., and P. C. Jordan. 1990. How does surface charge affect ion conduction and toxin binding in a sodium channel? *Biophysical Journal.* 57:883–891.

Dani, J. 1986. Ion-channel entrances influence permeation: net charge, size, shape, and binding considerations. *Biophysical Journal.* 49:607–618.

Drouin, H., and R. The. 1969. The effect of reducing extracellular pH on the membrane currents of the Ranvier node. *Pflügers Archiv.* 313:80–88.

Dubois, J. M., and C. Bergman. 1977. The steady-state potassium conductance of the Ranvier node at various external K-concentrations. *Pflügers Archiv.* 370:185–194.

Ermishkin, L. N., Kh. M. Kasumov, and V. M. Potseluyev. 1977. Properties of amphotericin B channels in a lipid bilayer. *Biochimica et Biophysica Acta.* 470:357–367.

Fernandez, J. M., A. P. Fox, and S. Krasne. 1984. Membrane patches and whole-cell membranes: a comparison of electrical properties in rat clonal pituitary ($GH_3$) cells. *Journal of Physiology.* 356:565–585.

French, R. J., and J. J. Shoukimas. 1985. An ion's view of the potassium channel: the structure of the permeation pathway as sensed by a variety of blocking ions. *Journal of General Physiology.* 85:669–698.

Gage, P. W., and D. Van Helden. 1979. Effects of permeant monovalent cations on end-plate channels. *Journal of Physiology.* 288:509–528.

Goldman, D. E. 1943. Potential, impedance, and rectification in membranes. *Journal of General Physiology.* 27:37–60.

Hille, B. 1968. Charges and potentials at the nerve surface. Divalent ions and pH. *Journal of General Physiology.* 51:221–236.

Hille, B. 1977. The pH-dependent rate of action of local anesthetics on the node of Ranvier. *Journal of General Physiology.* 69:475–496.

Hille, B., and W. Schwarz. 1978. Potassium channels as multi-ion single-file pores. *Journal of General Physiology.* 72:409–442.

Hodgkin, A. L., and A. F. Huxley. 1952, A quantitative description of membrane current and its application to conduction and excitation in nerve. *Journal of Physiology.* 117:500–544.

Hodgkin, A. L., and B. Katz. 1949. The effect of sodium ions on the electrical activity of the giant axon of the squid. *Journal of Physiology.* 108:37–77.

Hodgkin, A. L., and R. D. Keynes. 1955. The potassium permeability of a giant nerve fiber. *Journal of Physiology.* 128:61–88.

Jordan, P. C. 1987. How pore mouth charge distributions alter the permeability of transmembrane ionic channels. *Biophysical Journal.* 51:297–311.

Kolb, H. A., and E. Bamberg. 1977. Influence of membrane thickness and ion concentration on the properties of the gramicidin A channel. *Biochimica et Biophysica Acta.* 464:127–141.

Läuger, P. 1976. Diffusion-limited ion flow through pores. *Biochimica et Biophysica Acta.* 455:493–509.

Lucero, M. T., and P. A. Pappone. 1989. Voltage-gated potassium channels in brown fat cells. *Journal of General Physiology.* 93:451–472.

Marchais, D., and A. Marty. 1979. Interaction of permeant ions with channels activated by acetylcholine in *Aplysia* neurones. *Journal of Physiology.* 297:9–45.

Marty, A., and E. Neher. 1983. Tight-seal whole-cell recording. *In* Single Channel Recording. B. Sakmann and E. Neher, editors. Plenum Press, New York. 107–121.

Matteson, D. R., and R. P. Swenson, Jr. 1986. External monovalent cations that impede the closing of $K^+$ channels. *Journal of General Physiology.* 87:795–816.

Meves, H., and W. Vogel. 1973. Calcium inward currents in internally perfused giant axons. *Journal of Physiology.* 235:225–265.

Onodera, K., and A. Takeuchi. 1979. An analysis of the inhibitory post-synaptic current in the voltage-clamped crayfish muscle. *Journal of Physiology.* 286:265–282.

Plant, T. D. 1986. The effects of rubidium ions on components of the potassium conductance in the frog node of Ranvier. *Journal of Physiology.* 375:81–105.

Pusch, M., and E. Neher. 1988. Rates of diffusional exchange between small cells and a measuring patch pipette. *Pflügers Archiv.* 411:204–211.

Shapiro, M. S., and T. E. DeCoursey. 1988. Two types of potassium channels in a lymphoma cell line. *Biophysical Journal.* 53:550*a* (Abstr.)

Shapiro, M. S., and T. E. DeCoursey. 1989. Selectivity and permeant ion effects on gating in type *l* $K^+$ channels. *Biophysical Journal.* 55:200*a* (Abstr.)

Shapiro, M. S., and T. E. DeCoursey. 1991*a*. Mole-fraction dependence of slowing of tails by $Rb^+$ in mixtures of $K^+$ and $Rb^+$ provides further evidence that an external modulatory site regulates closing kinetics of type *l* $K^+$ channels. *Biophysical Journal.* 59:269*a*. (Abstr.)

Shapiro, M. S., and T. E. DeCoursey. 1991*b*. Selectivity and gating of the type *l* potassium channel in mouse lymphocytes. *Journal of General Physiology.* 97:1227–1250.

Spruce, A. E., N. B. Standen, and P. R. Stanfield. 1989. Rubidium ions and the gating of delayed rectifier potassium channels of frog skeletal muscle. *Journal of Physiology.* 411:597–610.

Swenson, R. P., Jr., and C. M. Armstrong. 1981. $K^+$ channels close more slowly in the presence of external $K^+$ and $Rb^+$. *Nature.* 291:427–429.

Van Helden, D., O. P. Hamill, and P. W. Gage. 1977. Permeant cations alter endplate channel characteristics. *Nature.* 269:711–713.

Yellen, G. 1984. Ionic permeation and blockade in $Ca^{2+}$-activated $K^+$ channels of bovine chromaffin cells. *Journal of General Physiology.* 84:157–186.